9-(4-Dimethylaminophenyl)benzo[b]quinolizinium: A Near-Infrared Fluorophore for the Multicolor Analysis of Proteins and Nucleic Acids in Living Cells

CHEMISTRY
A EUROPEAN JOURNAL

COMMUNICATION

DOI: 10.1002/chem.201301164

9-(4-Dimethylaminophenyl)benzo[*b*]quinolizinium: A Near-Infrared Fluorophore for the Multicolor Analysis of Proteins and Nucleic Acids in Living Cells

Roberta Bortolozzi,[a] Heiko Ihmels,*[b] Laura Thomas,[b] Maoqun Tian,[b] and Giampietro Viola*[a]

The visualization of cell components or processes within cells is an essential task in bioanalytical chemistry.[1] Specifically, the fluorimetric detection of biomacromolecules has developed as a key technique in this research area,[2] mainly because emission spectroscopy is a highly sensitive and straightforward method with relatively few demands on the equipment. As a consequence, several fluorescent probes have been established that enable the selective detection of cells or cellular components.[2–4] For example, DNA–fluorophore conjugates,[5] peptide-based molecular beacons,[6] groove-binding cyanine dyes,[7] and light-cleavable caged dyes[8] were shown to operate as DNA stains in live cells. Similarly, it was demonstrated that appropriately substituted metallointercalators have a high propensity to bind to cellular DNA and thus enable its fluorimetric detection,[2a,c,9] or, in some cases, the detection of other cell components.[10,11] The same principle was applied to detect RNA in nucleoli and the cytoplasm with a 2,7-carbazole derivative.[12] Furthermore, exciton-controlled hybridization-sensitive fluorescent oligonucleotide (ECHO) probes allow multicolor RNA imaging in cells.[13] Recently, a chemosensor has been presented that enables the fluorimetric differentiation of quadruplex DNA from other nucleic acids in cells.[14] Moreover, it has been shown that the fluorimetric discrimination of regions with different polarities may be accomplished in cells with quinoxaline derivatives.[15] Along these lines, the use of near-infrared (NIR, 650–900 nm) fluorescent probes is advantageous for biological applications, because NIR fluorophores exhibit low or almost no phototoxicity, relatively deep penetration into tissue, and negligible interference with the autofluorescence of cells.[16,17]

[a] Dr. R. Bortolozzi, Dr. G. Viola
Author names in alphabetical order
Dipartimento di Salute della Donna e del Bambino
Laboratorio di Oncoematologia
University of Padova, via Giustiniani 3, I-35128 Padova (Italy)
E-mail: giampietro.viola.1@unipd.it

[b] Prof. Dr. H. Ihmels, L. Thomas, Dr. M. Tian
Department Chemie–Biologie
Universität Siegen
Adolf-Reichwein-Strasse 2, 57068 Siegen (Germany)
E-mail: ihmels@chemie.uni-siegen.de

Supporting information for this article is available on the WWW under http://dx.doi.org/10.1002/chem.201301164.

We have shown recently that benzo[*b*]quinolizinium derivatives may be functionalized such that the fluorescence is quenched by different independent deactivation pathways and that the association with biomacromolecules results in light-up effects and shifts in the emission energy.[18] In some cases, separate deactivation channels enable the independent or even simultaneous detection of DNA and metal ions with one chemosensor.[19] In this context, we synthesized 9-(4-dimethylamino)benzo[*b*]quinolizinium (**1a**), which exhibits a very low emission quantum yield,[20] presumably caused by deactivation of the excited state by torsional relaxation and photoinduced electron transfer (PET) or charge shift (CS). Notably, some structural features of the derivative **1a** resemble aminophenylpyridinium derivatives such as **2**,[21] which have been used as fluorescent probes in nerve membranes,[22] and Thioflavin T (**3**), which has been applied for fluorimetric analysis of amyloid fibril formation.[23] Therefore, we proposed that the derivative **1a** may represent a complementary fluorimetric tool for the selective analysis of biomacromolecules, especially considering our experience with the benzo[*b*]quinolizinium ion as a ligand for DNA and proteins.[18,24] Herein, we demonstrate that different physiologically relevant host systems are stained with the chemosensor **1a**, most remarkably with different emission wavelengths and intensities. In addition, we show that, due to these properties, the chemosensor **1a** represents one of the rare examples of probes that stain cells with multicolored fluorescence.

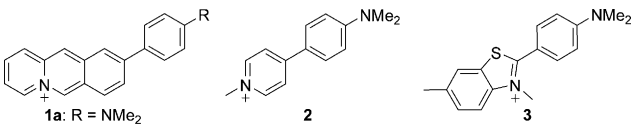

1a: R = NMe_2
1b: R = OMe

2 **3**

In aqueous solution, the benzo[*b*]quinolizinium derivative **1a** is essentially nonfluorescent ($\Phi_{FL} = 1.0 \times 10^{-3}$ in BPE buffer; see experimental section). However, we have shown already that the emission intensity increases significantly upon protonation, with a blueshifted fluorescence maximum.[20] The emission also increases with increasing viscosity of the solution (Figure 1, also see the Supporting Infor-

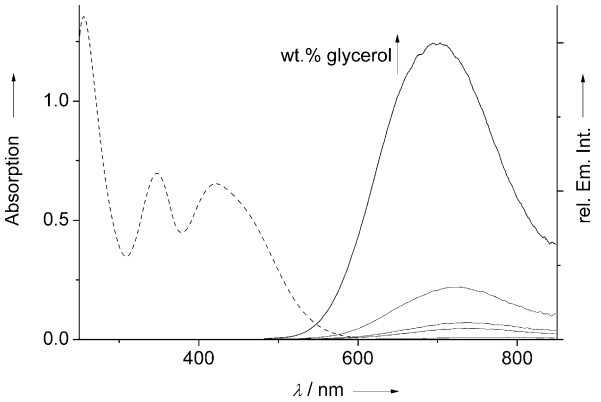

Figure 1. Absorption spectrum (dashed line) of **1a** (40 μM) in BPE buffer and emission spectra (continuous lines) of **1a** (40 μM) in glycerol–water mixtures (wt.% glycerol: 0, 40, 60, 80, 100%); $\lambda_{ex}=470$ nm; $T=20$°C; the arrow indicates changes in fluorescence intensity upon increasing the glycerol content from 0 to 100%.

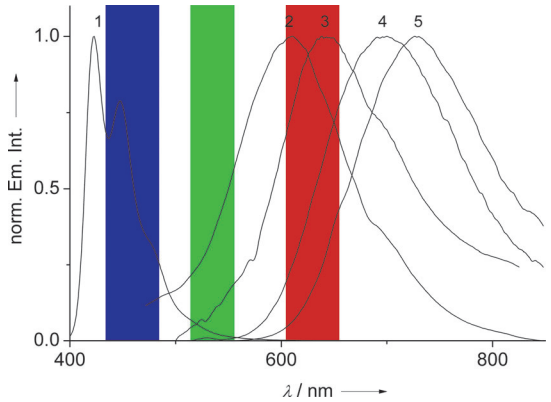

Figure 2. Normalized fluorescence spectra of **1a** in aqueous solution at pH 1.7 (1), or in the presence of BSA (2), quadruplex DNA **22AG** (4), ct DNA (5), and in the solid state (3); 1: $\lambda_{ex}=381$ nm; 2, 4: $\lambda_{ex}=421$ nm; 3, 5: $\lambda_{ex}=450$ nm; overlay: range of the filters used for cell experiments.

mation). Namely, upon excitation at $\lambda_{ex}=470$ nm, an intense redshifted emission band at 699 nm develops in glycerol–water mixtures as the glycerol content increases ($\Phi_{FL}=0.11$ in glycerol). The redshifted absorption and emission bands are characteristic of charge-transfer (CT) transitions, as expected for a donor–acceptor system such as **1a**. In addition, the CT bands appear to be sensitive towards the medium, because they are significantly redshifted as the glycerol content of the solution increases and eventually correspond to the bands observed in MeOH (see the Supporting Information). From these results, we deduce that the low emission quantum yield in homogeneous solution is mainly caused by conformational changes in the excited state, most likely by rotation about the biaryl axis, as clearly shown by the emission enhancement in viscous medium.[18b] Thus, in viscous media conformational changes are suppressed such that they are slower than the fluorescence, leading to an increase in the fluorescence quantum yield. However, the parent compound as well as the *p*-MeO-substituted derivative **1b** exhibit significantly higher emission quantum yields ($\Phi_{FL}=0.31$ and 0.29 in H_2O, respectively), and the protonation of the amino functionality alone causes an increase in the emission intensity of **1a**,[20] even without suppression of rotational freedom. These observations indicate that the torsional relaxation of the biaryl unit induces the deactivation of the excited **1a** only when it is accompanied by the formation of conformers that enable a charge shift (CS)[25] from the electron-donating aminophenyl fragment to the benzo[*b*]quinolizinium. As shown for derivatives **2** and **3**, and in general for donor–acceptor-substituted fluorophores,[25] this combination of a molecular twist and subsequent CS leads to the radiationless deactivation of the excited state.[21,23,25]

As the emission intensity of **1a** clearly depends on its conformational freedom, we examined the association with different host systems to assess whether the complex formation also leads to an increased emission intensity within the constrained environment of the binding site. Indeed, the addition of duplex or quadruplex DNA to compound **1a** led to significant changes in the fluorescence (Figures 2 and 3 and the Supporting Information). With double-stranded calf thymus DNA (ct DNA), an increase of the emission intensity by a factor of 38 was observed, with a maximum at 728 nm. In contrast, upon addition of the quadruplex-forming oligonucleotide 5′-A(GGGTTA)$_3$GGG-3′ (**22AG**), the emission intensity of **1a** increased by a factor of 96, and the emission maximum was redshifted to 697 nm.

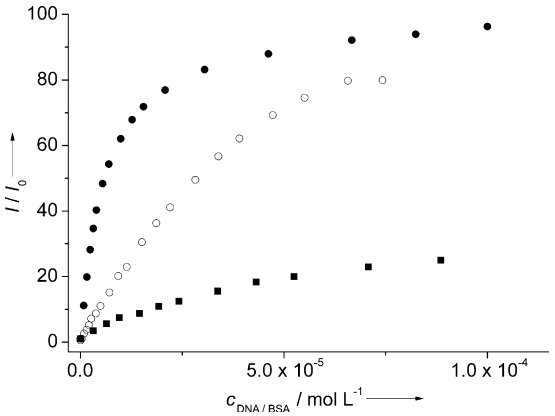

Figure 3. Change of the relative emission intensity, I/I_0, of **1a** (10 μM) upon addition of ct DNA (■) or BSA (○) in BPE buffer (10 mM, pH 7.0), or upon addition of quadruplex DNA **22AG** (●) in K-phosphate buffer (95 mM, pH 7.0).

Because the light-up effect of compound **1a** in the presence of DNA is likely caused by DNA binding, the association of ligand **1a** with duplex and quadruplex DNA was further investigated. Photometric titrations of ct DNA to **1a** revealed a DNA–ligand interaction, as evidenced by a hypochromic effect and a redshift of the absorption maximum (see the Supporting Information). The data of the photometric titrations were employed to determine the binding constant, $K_b=1.3\times10^4\,M^{-1}$, with a Scatchard plot.[26] The ab-

sence of clear isosbestic points as well as CD spectroscopic experiments indicate that more than two distinct absorbing species are formed during the photometric titration (see the Supporting Information). At low ligand/DNA ratios (0.08–0.2), a positive induced CD (ICD) signal was observed that is similar to the one of related intercalating benzo[*b*]quinolizinium derivatives.[18,19,24] In contrast, a bisignate ICD signal was observed at higher ligand/DNA ratios (0.2–1.0), which is characteristic of an exciton coupling[27] resulting from ligands that aggregate along the DNA backbone.[28]

The interaction of quadruplex DNA with compound **1a** was examined with thermal denaturation experiments with the dye-labeled quadruplex-forming oligonucleotide fluorescein-$(GGGTTA)_3GGG$-tetramethyrhodamine (**F21T**) (FRET melting, FRET = Förster resonance energy transfer).[29] With increasing ligand/DNA ratios (0, 0.25, 0.5, 1, 5), the quadruplex **F21T** is stabilized against dissociative unfolding, as indicated by the increasing melting temperature ΔT_m (see the Supporting Information), although it should be noted that this ΔT_m value denotes a relatively weak stabilization.[29] Complementary CD spectroscopic studies confirmed the association of ligand **1a** with quadruplex DNA (see the Supporting Information), because the addition of **1a** to **22AG** led to a change of the CD spectrum. The initial spectrum shows the typical signal pattern of a mixture of parallel and antiparallel quadruplex forms and consists of maxima at 210, 250, and 290, a weak shoulder at 270, and a minimum at 235 nm. Upon addition of **1a**, the maximum at 295 nm and the shoulder at 270 nm increased, and the signal at 235 nm was maintained with a slightly increased intensity. In addition, a maximum at 245 nm and a minimum at 265 nm developed with increasing ligand/DNA ratios to give an overall CD signature that is characteristic of an antiparallel quadruplex DNA structure.[30] These results indicate that the ligand **1a** stabilizes this particular quadruplex form upon association. Furthermore, a weak ICD signal was observed in the absorption range of the ligand **1a** that results from dipole–dipole interactions between the ligand and chiral quadruplex DNA and provides further evidence of the association of **1a** with **22AG**.[29] Furthermore, the bisignate form of the ICD band indicates external stacking of ligands along the phosphate backbone, which was confirmed by a Job plot from fluorimetric data that revealed a ligand/DNA stoichiometry of 3:1 (see the Supporting Information). Moreover, a binding constant of $K_b = 8.3 \times 10^4\,M^{-1}$ was obtained from the Scatchard-plot analysis[26] of the fluorimetric titration. These data show that **1a** binds to quadruplex DNA, similar to other cationic hetarene-type ligands.[31]

As compared with nucleic acids, the addition of a representative protein, namely bovine serum albumin (BSA), to the quinolizinium derivative **1a** resulted in a redshifted emission maximum at 609 nm with a light-up factor of 80 (Figures 2 and 3). At the same time, a hypochromic effect and a slight blueshift of the absorption maximum were observed during photometric titration (see the Supporting Information). The association of **1a** with the protein was further examined by CD spectroscopy. Upon addition of **1a** to BSA, the intensity of the negative CD absorption bands of the protein decreased. Moreover, a weak ICD band of the ligand at high ligand concentrations indicated the association of **1a** with BSA (see the Supporting Information). To show that the increasing emission intensity of **1a** is the result of its association with BSA, fluorimetric displacement experiments were performed.[32] The ligand **1a** does not interfere with the association of dansyl proline, a site II selective ligand, with BSA, but the addition of dansylamide, a site I selective ligand, to a mixture **1a** and BSA resulted in a clear displacement of **1a** from its binding site, as indicated by the decrease of the fluorescence intensity of **1a** (see the Supporting Information).

Overall, the results summarized above indicate that the association of the ligand **1a** with appropriate host systems results in a strong increase of the emission intensity. As has been shown for several fluorescent probes,[33] and in particular for benzo[*b*]quinolizinium derivatives,[18] this light-up effect of **1a** in the presence of a host molecule is likely the result of the suppressed deactivation pathways in the excited state, mainly due to reduced conformational flexibility within the binding site. The most interesting feature of the ligand **1a** is the strong dependence of the emission wavelength and of the emission intensity on the particular host system. A similar polychromic effect has been for observed with acridine orange, which exhibits different emission colors when bound to double-stranded DNA or single-stranded RNA,[34] or with fluorescent ligands that emit with dissimilar fluorescence maxima in the presence of regular duplex DNA or abasic-site-containing DNA.[35] Also, a dinuclear Ru^{II} complex has been reported whose emission maximum is blueshifted when bound to quadruplex DNA, as compared to the complex with duplex DNA.[36] Most notably, the shift of the emission maximum of this compound varies with different quadruplex DNA forms.[37] In all cases mentioned above, it has been proposed that the changes of the emission properties in different host systems originate from different binding modes of the fluorescent ligand in the particular binding site. Therefore, we conclude that the variation in the emission properties of **1a** in different host systems is also induced by different types of association of the ligand in each binding site.

It may be considered as well that aggregation alone could induce redshifted emission for **1a**, as shown for several J-aggregated cationic dyes.[38] However, since the spectra of **1a** in BSA or DNA do not resemble the one obtained in the solid state ($\lambda_{Fl} = 642$ nm, see Figure 2), aggregation is obviously not a main factor that determines the emission properties in these constrained media.

The analysis of the emission colors of **1a** in different binding sites shows that the fluorescence bands overlap with the wavelength ranges of commonly employed fluorescence microscopes (see colored areas in Figure 2), thus potentially enabling a multicolor analysis of separate sites of probe localization in one sample. Therefore, we examined whether the probe **1a** may be used for fluorimetric differentiation of distinct cell components. For that purpose, HeLa cells were

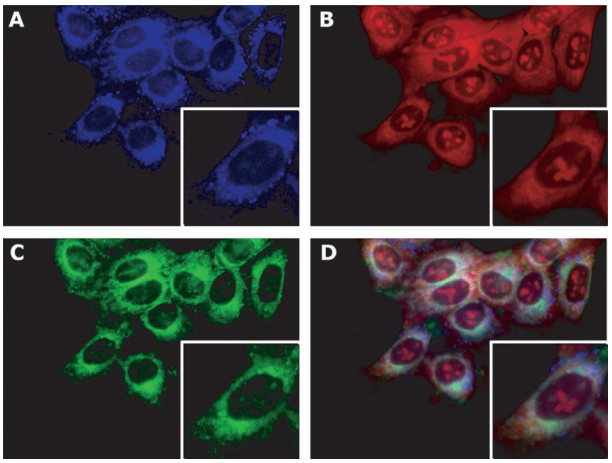

Figure 4. Fluorescence micrographs of HeLa cells after incubation with 1a (2.5 μm) for 1 h. Pictures were taken with a video confocal microscope (Nikon Eclipse 80i; Nikon Nir Apo 60X/1.0W water immersion objective). The different emission colors were separated by blocking filters. The insets in the panels represent an enlargement of one cell for better visualization of the dye disposition inside the cells. Panel A: $\lambda_{ex}=350$–400 nm, $\lambda_{Fl}=435$–485 nm; panel B: $\lambda_{ex}=540$–565 nm, $\lambda_{Fl}=605$–655 nm; panel C: $\lambda_{ex}=465$–495 nm, $\lambda_{Fl}=515$–555 nm; panel D: overlay of all pictures.

treated with **1a** (2.5 μM), and after 1 h of incubation, the cells were examined with a confocal fluorescence microscope (Figure 4). Notably, varying the filter systems revealed a remarkable multicolor picture that did not change with longer incubation times. Namely, the nucleoli exhibited a red emission, whereas in the cytoplasm red, blue, and green fluorescent areas were detected. We interpret this behavior as a combination of the photophysical properties of **1a**: 1) the formation of differently absorbing and emitting conformers, 2) the dependence of the emission on the excitation wavelength, and 3) the strong influence of the environment on the emission color. Most likely, the punctuate blue emission originates from probe molecules in the lysosomes (Figure 4, panel A), because the low pH in these organelles leads to protonation of **1a** ($pK_a=3.8$).[20] Considering the redshift of the emission of **1a** in the presence of nucleic acids, we propose that the red emission in the nuclei results from DNA-bound ligands, whereas the red emission in the cytoplasm may originate from the association of the ligand with double-stranded regions of RNA or proteins in this medium. At the same time, the green emission in the cytoplasm may result from binding of **1a** to proteins, because, at least when bound to BSA, **1a** exhibits significant emission in the applied filter range (515–555 nm). Most notably, the superposition of the different fluorescence pictures (Figure 4, panel D) reveals several fine structures showing that at higher resolutions a multicolor-based differentiation of cell components may be accomplished.

In summary, we demonstrated that the emission properties of 9-(4-dimethylamino)benzo[*b*]quinolizinium (**1a**) depend on the surrounding microenvironment and that this property may be used for the fluorimetric differentiation of biologically relevant host systems. Notably, the fluorophore emits in the NIR region, which is a favorable property for fluorescent probes for bioanalytical applications. Although detailed photophysical studies are still necessary to clarify the complete mechanism of this remarkable effect, it is shown already in these preliminary experiments that **1a** represents one of the few chemosensors that enables a multicolor fluorimetric analysis of living cells.

Experimental Section

Materials: Purified water with resistivity $\geq 18\,M\Omega\,cm^{-1}$ was used for the preparation of buffer solutions and spectrometric measurements. BPE buffer (6.0 mM Na_2HPO_4, 2.0 mM NaH_2PO_4, 1.0 mM Na_2EDTA; total Na^+ concentration 16.0 mM; pH 7.0) was used for photometric ct DNA and BSA titrations and for CD spectroscopic studies with ct DNA and BSA. K-phosphate buffer (25 mM KH_2PO_4, 25 mM K_2HPO_4, 70 mM KCl; pH 7.0) was used for photometric DNA titrations and for CD spectroscopic studies with the quadruplex-forming DNA sequence **22AG**. The cacodylate buffer (10 mM KCl, 90 mM LiCl, 10 mM Na-cacodylate; pH 7.2) was used for DNA melting experiments. Buffer solutions were filtered through a PVDF membrane filter (pore size 0.45 μm) prior to use. UV/Vis spectra were recorded using a Varian Cary 100 Bio spectrophotometer; fluorescence spectra were recorded on a Varian Cary Eclipse spectrofluorometer. For the CD spectroscopic experiments a Chirascan CD spectrometer from Applied Photophysics was used. Calf thymus DNA was purchased from Sigma (St. Louis, USA). The quadruplex-forming sequences $(AG_3T_2)_3AG_3$ (**22AG**) and fluo-$G_3(T_2AG_3)_3$-tamra (**F21T**) were purchased from Metabion International AG (Martinsried, Germany). Bovine serum albumin was purchased from Fluka Chemie AG (Buchs, Switzerland).

Spectrophotometric and spectrofluorimetric titrations: All spectrometric measurements were performed in thermostated quartz sample cells (10 mm pathlength) at 20 °C. Solutions for analysis were prepared from stock solutions in methanol shortly before the experiments. To avoid effects from the co-solvents, aliquots of the stock solution of the ligand were pipetted into vials, the solvent was evaporated and the residue was dissolved in the corresponding buffer. To avoid dilution of the analyte solutions during titration, the titrant solutions contained DNA and the ligand at the same concentration as in the analyte solution. The actual concentrations of the ct DNA samples were determined photometrically using the extinction coefficient $\varepsilon_{260}=12824\,cm^{-1}\,M^{-1}$ (bp). Aliquots of the analyte solutions were placed into quartz cells and titrated with the titrant solutions in intervals of 0.5–2 equivalents, and absorption or emission spectra were recorded. The titrations were stopped after no changes were observed in the absorption or emission spectra upon addition of at least three two-equivalent portions of the titrant. All spectrometric titrations were performed at least three times to ensure the reproducibility. The excitation wavelengths are given in the legends for each titration. In cases where the absorbance changes significantly at this wavelength, the emission spectra were corrected against the absorption. Emission spectra in the range between 600 and 800 nm were corrected using an instrument-specific correction curve.

Cell culture and fluorescence microscopy: The human cervical adenocarcinoma (HeLa) cell line was purchased from the American Type Culture Collection. The cells were grown in Dulbecco's modified Eagle's medium (Invitrogen, Milano, Italy), supplemented with 10% heat-inactivated fetal bovine serum, 100 U/mL penicillin G and 10 $\mu g\,mL^{-1}$ streptomycin at 37 °C in a humidified incubator with 5% CO_2. The cells were incubated with compound **1a** in complete medium for 1 h, and then the medium was discarded and replaced by Hank's Balanced Salt Solution (HBSS). Fluorescent micrographs were taken with a video confocal microscope (Nikon Eclipse 80i, Melville, NY, USA), using a Nikon Nir Apo 60X/1.0W water immersion objective.

Acknowledgements

Generous support by the Deutsche Forschungsgemeinschaft (FOR516) is gratefully acknowledged. We thank Prof. Dr. Karl-Heinz Drexhage and Dr. Jutta Arden-Jacob, Physical Chemistry, University of Siegen, for the generous donation of Oxazine 170.

Keywords: DNA · emission spectroscopy · fluorescent probes · imaging agents

[1] L. J. Kricka, P. Fortina, *Clin. Chem.* **2009**, *55*, 670–683.

[2] a) K. K.-W. Lo, A. W.-T. Choi, W. H.-T. Law, *Dalton Trans.* **2012**, *41*, 6021–6047; b) S. Yao, K. D. Belfield, *Eur. J. Org. Chem.* **2012**, 3199–3217; c) M. R. Gill, J. A. Thomas, *Chem. Soc. Rev.* **2012**, *41*, 3179–3192; d) P. V. Chang, C. R. Bertozzi, *Chem. Commun.* **2012**, *48*, 8864–8879; e) S. Wilmes, M. Staufenbiel, D. Liße, C. P. Richter, O. Beutel, K. B. Busch, S. T. Hess, J. Piehler, *Angew. Chem.* **2012**, *124*, 4952–4955; *Angew. Chem. Int. Ed.* **2012**, *51*, 4868–4871; f) B. Juskowiak, *Anal. Bioanal. Chem.* **2011**, *399*, 3157–3176; g) H. Kobayashi, M. Ogawa, R. Alford, P. L. Choyke, Y. Urano, *Chem. Rev.* **2010**, *110*, 2620–2640; h) T. R. Gingeras, R. Higuchi, L. J. Kricka, Y. M. D. Lo, C. T. Wittwer, *Clin. Chem.* **2005**, *51*, 661–671.

[3] S. Zhang, C. Yang, W. Zhu, B. Zeng, Y. Yang, Y. Xu, X. Qian, *Org. Biomol. Chem.* **2012**, *10*, 1653–1658.

[4] T. E. McCann, N. Kosaka, Y. Koide, M. Mitsunaga, P. L. Choyke, T. Nagano, Y. Urano, H. Kobayashi, *Bioconjugate Chem.* **2011**, *22*, 2531–2538.

[5] a) Y. N. Teo, E. T. Kool, *Chem. Rev.* **2012**, *112*, 4221–4245; b) C. Holzhauser, S. Berndl, F. Menacher, M. Breunig, A. Göpferich, H.-A. Wagenknecht, *Eur. J. Org. Chem.* **2010**, 1239–1248; c) H.-A. Wagenknecht, *Ann. N. Y. Acad. Sci.* **2008**, *1130*, 122–130.

[6] J. Wu, Y. Zou, C. Li, W. Sicking, I. Piantanida, T. Yi, C. Schmuck, *J. Am. Chem. Soc.* **2012**, *134*, 1958–1961.

[7] X. Peng, T. Wu, J. Fan, J. Wang, S. Zhang, F. Song, S. Sun, *Angew. Chem.* **2011**, *123*, 4266–4269; *Angew. Chem. Int. Ed.* **2011**, *50*, 4180–4183.

[8] a) M. I. Sánchez, J. Martínez-Costas, F. Gonzalez, M. A. Bermudez, M. E. Vázquez, J. L. Mascareñas, *ACS Chem. Biol.* **2012**, *7*, 1276–1280; b) M. A. Priestman, T. A. Shell, L. Sun, H.-M. Lee, D. S. Lawrence, *Angew. Chem.* **2012**, *124*, 7804–7807; *Angew. Chem. Int. Ed.* **2012**, *51*, 7684–7687.

[9] a) R. B. P. Elmes, M. Erby, S. A. Bright, D. C. Williams, T. Gunnlaugsson, *Chem. Commun.* **2012**, *48*, 2588–2590; b) F. L. Thorp-Greenwood, M. P. Coogan, L. Mishra, N. Kumari, G. Rai, S. Saripella, *New J. Chem.* **2012**, *36*, 64–72; c) F. L. Thorp-Greenwood, *Organometallics* **2012**, *31*, 5686–5692; d) M. Matson, F. R. Svensson, B. Nordén, P. Lincoln, *J. Phys. Chem. B* **2011**, *115*, 1706–1711; e) C. Li, M. Yu, Y. Sun, Y. Wu, C. Huang, F. Li, *J. Am. Chem. Soc.* **2011**, *133*, 11231–11239.

[10] V. Pierroz, T. Joshi, A. Leonidova, C. Mari, J. Schur, I. Ott, L. Spiccia, S. Ferrari, G. Gasser, *J. Am. Chem. Soc.* **2012**, *134*, 20376–20387.

[11] R. B. P. Elmes, K. N. Orange, S. M. Cloonan, D. C. Williams, T. Gunnlaugsson, *J. Am. Chem. Soc.* **2011**, *133*, 15862–15865.

[12] X. Liu, Y. Sun, Y. Zhang, F. Miao, G. Wang, H. Zhao, X. Yu, H. Liu, W.-Y. Wong, *Org. Biomol. Chem.* **2011**, *9*, 3615–3618.

[13] A. Okamoto, *Chem. Soc. Rev.* **2011**, *40*, 5815–5828.

[14] Y.-J. Lu, S.-C. Yan, F.-Y. Chan, L. Zou, W.-H. Chung, W.-L. Wong, B. Qiu, N. Sun, P.-H. Chan, Z.-S. Huang, L.-Q. Gu, K.-Y. Wong, *Chem. Commun.* **2011**, *47*, 4971–4973.

[15] K. Kudo, A. Momotake, J. K. Tanaka, Y. Miwa, T. Arai, *Photochem. Photobiol. Sci.* **2012**, *11*, 674–678.

[16] a) L. Yuan, W. Lin, K. Zheng, L. He, W. Huang, *Chem. Soc. Rev.* **2013**, *42*, 622–661; b) Y.-Q. Sun, J. Liu, X. Lv, Y. Liu, Y. Zhao, W. Guo, *Angew. Chem.* **2012**, *124*, 7752–7754; *Angew. Chem. Int. Ed.* **2012**, *51*, 7634–7636.

[17] G. Lukinavičius, K. Umezawa, N. Olivier, A. Honigmann, G. Yang, T. Plass, V. Mueller, L. Reymond, I. R. Corrêa Jr, Z.-G. Luo, C. Schultz, E. A. Lemke, P. Heppenstall, C. Eggeling, S. Manley, K. Johnsson, *Nat. Chem.* **2013**, *5*, 132–139.

[18] a) K. Faulhaber, A. Granzhan, H. Ihmels, D. Otto, L. Thomas, S. Wells, *Photochem. Photobiol. Sci.* **2011**, *10*, 1535–1545; b) A. Granzhan, H. Ihmels, G. Viola, *J. Am. Chem. Soc.* **2007**, *129*, 1254–1267; c) K. Faulhaber, A. Granzhan, H. Ihmels, G. Viola, *Pure Appl. Chem.* **2006**, *78*, 2325–2335; d) A. Granzhan, H. Ihmels, *Org. Lett.* **2005**, *7*, 5119–5122.

[19] a) M. Tian, H. Ihmels, S. Ye, *Org. Biomol. Chem.* **2012**, *10*, 3010–3018; b) M. Tian, H. Ihmels, K. Benner, *Chem. Commun.* **2010**, *46*, 5719–5721.

[20] M. Tian, H. Ihmels, *Synthesis* **2009**, 4226–4234.

[21] a) G. Hübener, A. Lambacher, P. Fromherz, *J. Phys. Chem. B* **2003**, *107*, 7896–7902; b) V. Kharlanov, W. Rettig, *Chem. Phys.* **2007**, *332*, 17–26; c) W. Rettig, V. Kharlanov, M. Maus, *Chem. Phys. Lett.* **2000**, *318*, 173–180; d) P. Fromherz, A. Heileman, *J. Phys. Chem.* **1992**, *96*, 6864–6866; e) H. Ephardt, P. Fromherz, *J. Phys. Chem.* **1991**, *95*, 6792–6797.

[22] a) D. Braun, P. Fromherz, *Biophys. J.* **2004**, *87*, 1351–1359; b) B. Kuhn, P. Fromherz, W. Denk, *Biophys. J.* **2004**, *87*, 631–639; c) P. Fromherz, T. Vetter, *Proc. Natl. Acad. Sci. USA* **1992**, *89*, 2041–2045; d) L. M. Loew, L. L. Simpson, *Biophys. J.* **1981**, *34*, 353–365; e) A. Grinvald, R. Hildesheim, I. D. Farber, L. Anglister, *Biophys. J.* **1982**, *39*, 301–308.

[23] a) N. Amdursky, Y. Erez, D. Huppert, *Acc. Chem. Res.* **2012**, *45*, 1548–1557; b) A. I. Sulatskaya, A. A. Maskevich, I. M. Kuznetsova, V. N. Uversky, K. K. Turoverov, *PLoS ONE* **2010**, *5*, e15385; c) V. I. Stsiapura, A. A. Maskevich, S. A. Tikhomirov, O. V. Buganov, *J. Phys. Chem. A* **2010**, *114*, 8345–8350; d) P. K. Singh, M. Kumbhakar, H. Pal, S. Nath, *J. Phys. Chem. B* **2010**, *114*, 5920–5927; e) H. LeVine, *Methods Enzymol.* **1999**, *309*, 274–284; f) H. Naiki, K. Higuchi, M. Hosokawa, T. Takeda, *Anal. Biochem.* **1989**, *177*, 244–249.

[24] H. Ihmels, K. Faulhaber, D. Vedaldi, F. Dall′Acqua, G. Viola, *Photochem. Photobiol.* **2005**, *81*, 1107–1115.

[25] a) Z. R. Grabowski, K. Rotkiewicz, *Chem. Rev.* **2003**, *103*, 3899–4031; b) C. Prunkl, M. Pichlmaier, R. Winter, V. Kharlanov, W. Rettig, H.-A. Wagenknecht, *Chem. Eur. J.* **2010**, *16*, 3392–3402.

[26] F. H. Stootman, D. M. Fisher, A. Rodger, J. R. Aldrich-Wright, *Analyst* **2006**, *131*, 1145–1151.

[27] a) B. Nordén, T. Kurucsev, *J. Mol. Recognit.* **1994**, *7*, 141–156.

[28] H. Ihmels, K. Faulhaber, C. Sturm, G. Bringmann, K. Messer, N. Gabellini, D. Vedaldi, G. Viola, *Photochem. Photobiol.* **2001**, *74*, 505–511.

[29] A. De Cian, L. Guittat, M. Kaiser, B. Sacca, S. Amrane, A. Bourdoncle, P. Alberti, M. P. Teulade-Fichou, L. Lacroix, J. L. Mergny, *Methods* **2007**, *42*, 183–195.

[30] a) E. M. Rezler, J. Seenisamy, S. Bashyam, M.-Y. Kim, E. White, D. Wilson, L. H. Hurley, *J. Am. Chem. Soc.* **2005**, *127*, 9439–9447; b) J. Kypr, I. Kejnovská, D. Renčiuk, M. Vorlíčková, *Nucl. Acids Res.* **2009**, *37*, 1713–1725; c) M. Vorlíčková, I. Kejnovská, J. Sagi, D. Renčiuk, K. Bednářová, J. Motlová, J. Kypr, *Methods* **2012**, *57*, 64–75.

[31] a) J. L.-Y. Chen, J. Sperry, N. Y. Ip, M. A. Brimble, *Med. Chem. Commun.* **2011**, *2*, 229–245; b) S. N. Georgiades, N. H. Abd Karim, K. Suntharalingam, R. Vilar, *Angew. Chem.* **2010**, *122*, 4114–4128; *Angew. Chem. Int. Ed.* **2010**, *49*, 4020–4034; c) T.-M. Ou, Y.-J. Lu, J.-H. Tan, Z.-S. Huang, K.-Y. Wong, L.-Q. Gu, *ChemMedChem* **2008**, *3*, 690–713; d) D. Monchaud, M.-P. Teulade-Fichou, *Org. Biomol. Chem.* **2008**, *6*, 627–636.

[32] V. S. Jisha, K. T. Arun, M. Hariharan, D. Ramaiah, *J. Phys. Chem. B* **2010**, *114*, 5912–5919.

[33] a) R. N. Dsouza, U. Pischel, W. M. Nau, *Chem. Rev.* **2011**, *111*, 7941–7980; b) A. Hawe, M. Sutter, W. Jiskoot, *Pharm. Res.* **2008**, *25*, 1487–1499; c) J. R. Lakowicz, *Principles of Fluorescence Spectroscopy,* 3rd ed., Plenum Publishing, New York, **2006**.

[34] a) "Acridine orange: A versatile probe of nucleic acids and other cell constituents": Z. Darzynkiewicz, J. Kapuscinski in *Flow Cytome-*

try and Sorting (Eds.: M. R. Melamed, T. Lindmo, M. L. Mendelsohn), Wiley, New York, **1990**, pp. 291–314; b) G. Löber, *J. Lumin.* **1981**, *22*, 221–265.

[35] a) F. Wu, Y. Shao, K. Ma, Q. Cui, G. Liu, S. Xu, *Org. Biomol. Chem.* **2012**, *10*, 3300–3307; b) A. Fakhari M, S. E. Rokita, *Chem. Commun.* **2011**, *47*, 4222–4224.

[36] C. Rajput, R. Rutkaite, L. Swanson, I. Haq, J. A. Thomas, *Chem. Eur. J.* **2006**, *12*, 4611–4619.

[37] T. Wilson, M. P. Williamson, J. A. Thomas, *Org. Biomol. Chem.* **2010**, *8*, 2617–2621.

[38] M. Levitus, S. Ranjit, *Quart. Rev. Biophys.* **2011**, *44*, 123–151.

Received: March 26, 2013
Published online: ■■ ▮▮, 0000

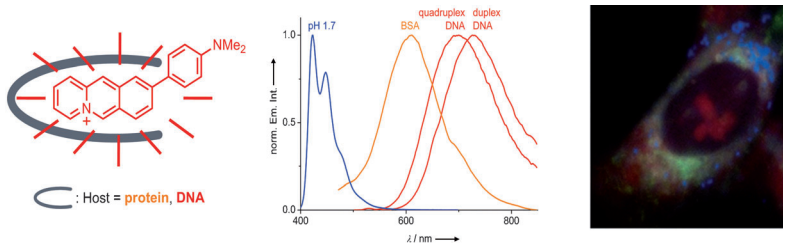

All lit up: The title compound operates as a fluorescent light-up probe that enables the detection of different biologically relevant hosts at different fluorescence maxima. It is demonstrated that this chemosensor also allows the fluorimetric multicolor analysis of different components in living cells (see figure).

Fluorescent Probes

R. Bortolozzi, H. Ihmels, L. Thomas, M. Tian, G. Viola** ..... ▮▮▮▮–▮▮▮▮

9-(4-Dimethylaminophenyl)benzo[*b*]-quinolizinium: A Near-Infrared Fluorophore for the Multicolor Analysis of Proteins and Nucleic Acids in Living Cells